Applied Catalysis A: General 400 (2011) 142–147

Contents lists available at ScienceDirect

Applied Catalysis A: General

journal homepage: www.elsevier.com/locate/apcata

Solvent effects on $Cu_2O(1\,1\,1)$ surface properties and CO adsorption on $Cu_2O(1\,1\,1)$ surface: A DFT study

Riguang Zhang, Lixia Ling, Zhong Li, Baojun Wang*

Key Laboratory of Coal Science and Technology of Ministry of Education and Shanxi Province, Taiyuan University of Technology, No. 79 Yingze West Street, Taiyuan 030024, Shanxi, China

ARTICLE INFO

Article history:
Received 9 December 2010
Received in revised form 3 April 2011
Accepted 20 April 2011
Available online 29 April 2011

Keywords:
Carbon monoxide
$Cu_2O(1\,1\,1)$
Adsorption
Solvent effect
Density functional theory

ABSTRACT

Based on density functional theory, together with COSMO (conductor-like solvent model) in Dmol^3, the solvent effects on both the $Cu_2O(1\,1\,1)$ surface properties and the adsorption of CO on $Cu_2O(1\,1\,1)$ surface have been systematically investigated. Different dielectric constants, including vacuum, liquid paraffin, methylene chloride, methanol and water, are considered. The solvent effect on $Cu_2O(1\,1\,1)$ surface properties shows that the solvent favors $Cu_2O(1\,1\,1)$ surface area growth. The adsorption of CO on $Cu_2O(1\,1\,1)$ surface indicates that the structural parameters and adsorption energies of CO are very sensitive to the COSMO solvent model. Solvent effects can effectively improve the stability of CO adsorption on $Cu_2O(1\,1\,1)$ surface and the case of C–O bond activation. The interaction of solvent molecules with $Cu_2O(1\,1\,1)$ surface is compared with that of CO with $Cu_2O(1\,1\,1)$. Results suggest that the solvent effect is the dominating cause for the interaction of CO with $Cu_2O(1\,1\,1)$ surface in solvent, in which $Cu_2O(1\,1\,1)$ shows higher catalytic activity for CO activation. But the solvent may be not the only reason promoting CO activation. These analyses give us some new insights into the understanding of solvent effects.

1. Introduction

The formation of dimethyl ether (DME) and methanol from syngas ($CO + H_2$) conversion has recently attracted more and more attention, because the materials can be used as an alternative diesel fuel or as a fuel additive [1,2]. There are two methods of "one-pot" synthesis of DME: the gas phase method and the liquid-phase method. The gas phase method generally uses a fixed bed reactor [3–6]. The liquid-phase method uses a slurry reactor, in which the catalyst is dispersed in an inert liquid medium such as liquid paraffin [7–10]. The gas–slurry process shows the following advantages relative to the conventional gas–solid processes: excellent temperature control, no diffusion limitations, low pressure drop over the reactor, low gas recycle ratio and efficient energy economy. Therefore, the liquid-phase method in a slurry reactor has been considered as one of the most promising methods for DME formation.

Copper has been considered as a potential substitute for noble metals because of its low cost and high activity for CO and H_2 in the "one-pot" synthesis of DME [11–14]. However, the active center of copper has been a matter of debate in the literature over the past two decades [15–18]. We shall not take part in this debate here. Sheffer et al. [15], Herman et al. [17] and Zuo et al. [19] have found that Cu_2O shows higher catalytic activity than Cu.

Because the details about the interaction of small molecules with catalyst surfaces are important to understand the surface structure of catalyst and the catalytic processes, up to now, the adsorption of CO with Cu_2O in gas phase has been studied by many researchers [20–24]; such adsorption is thought to be the first step in the synthetic procedure. Meanwhile, many studies have shown that the chemical characteristics in liquid phase environment are different from those in gas phase, namely, the utilization environments of catalyst might change the structure and activity of the catalyst, in which the solvent environment plays an important role [25–28]. To our knowledge, a detailed understanding of the general rules involving Cu_2O properties and the interaction of CO with Cu_2O surfaces in different liquid phase environments, as well as the role of solvent in corresponding solvent environments has seldom been presented. So the Dmol^3 implementation of the COSMO (conductor-like screening model) is applied to simulate the dielectric response of the solvent environment [29–32]. The COSMO model, which can well describe the solvent effect, has been used to investigate solvent effects on CO adsorption over $CuCl(1\,1\,1)$ surface in our previous studies [33].

XRD characterization has proved that $Cu_2O(1\,1\,1)$ surface is the main surface of Cu_2O [34,35]. In this study, we report a systematic COSMO-based DFT investigation about $Cu_2O(1\,1\,1)$ surface properties in different solvent environments and the interaction of CO

* Corresponding author. Tel.: +86 351 6018539; fax: +86 351 6041237.
E-mail addresses: wangbaojun@tyut.edu.cn, quantumtyut@126.com (B. Wang).

0926-860X/$ – see front matter © 2011 Elsevier B.V. All rights reserved.
doi:10.1016/j.apcata.2011.04.025

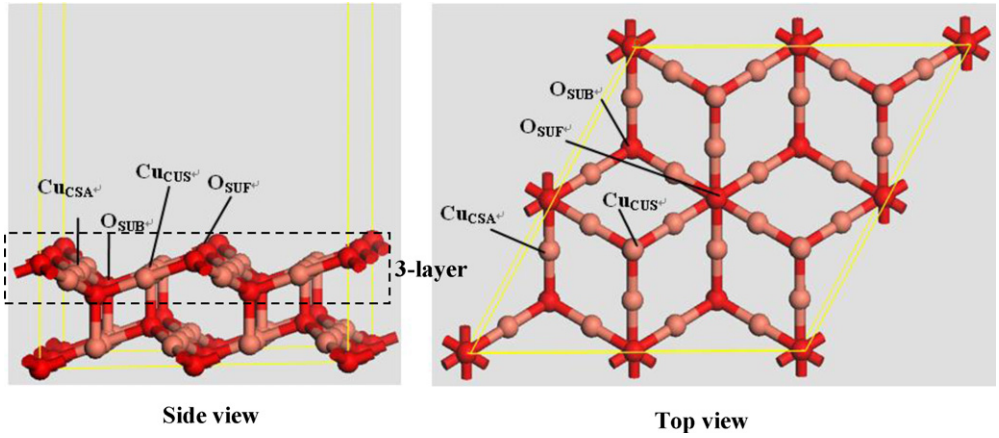

Fig. 1. $Cu_2O(1\,1\,1)$–2×2 supercell. Orange and red balls stand for Cu and O atoms throughout the paper. (For interpretation of the references to color in this figure legend, the reader is referred to the web version of the article.)

with $Cu_2O(1\,1\,1)$ in different solvent environments. Values of the solvent dielectric constants ε ranging from 2.06 (liquid paraffin) to 78.54 (water) are considered, including 9.08 (methylene chloride) and 32.63 (methanol). COSMO has not been used in vacuum (gas phase) ($\varepsilon = 1$). The calculated results are expected to illustrate the role of the solvent and to give some new insights into the solvent effect on the stability and the activity of Cu_2O catalyst, as well as the activation ability of CO on $Cu_2O(1\,1\,1)$ surface.

2. Computation models and methods

The $Cu_2O(1\,1\,1)$ surfaces are modeled by using the supercell approach, where periodic boundary conditions are applied to the central supercell so that it is reproduced periodically throughout space. The ideal and perfect $Cu_2O(1\,1\,1)$ surface is non-polar; it includes four chemically different types of surface atoms, which are denoted as Cu_{CUS}, Cu_{CSA}, O_{SUF} and O_{SUB}, as shown in Fig. 1. Cu_{CUS} is the surface copper that is coordinatively unsaturated, i.e., singly coordinate Cu^+ cations. Cu_{CSA} is the coordinatively saturated copper atom, i.e., doubly coordinate Cu^+. O_{SUF} is the outer-most surface oxygen, i.e., threefold-coordinate oxygen anions. And O_{SUB} is the subsurface oxygen, i.e., fourfold-coordinate oxygen anions.

Our calculations on $Cu_2O(1\,1\,1)$–2×2 surface have been done by using slab models of six layers. The vacuum gap is set to 1 nm, at such a distance there is little interaction between the neighboring layers. The adsorbate and the three outermost atomic layers of the substrate are allowed to relax in all of the geometry optimization calculations (allowed to move in any direction according to forces), and the three bottom-most atomic layers of the substrate are kept fixed to the bulk coordinates [36].

The exchange and correlation effects are described through the generalized gradient approximation (GGA) of Becke–Lee–Yang–Parr (BLYP) [37,38]. The double numeric basis with polarization functions (DNP) is used for all atoms in the adsorbed and substrate systems [39]. All electron basis set is used for C and O atoms, and effective core potentials (ECP) are used for Cu atoms [40]. Brillouin-zone integrations have been performed using a $2 \times 2 \times 1$ Monkhorst-Pack grid and a Methfessel–Paxton smearing of 0.005 Ha. The convergence criteria judged by the energy, force and displacement, respectively, are 2×10^{-5} Ha, 4×10^{-3} Ha/Å and 5×10^{-3} Å. All calculations are carried out with the Dmol^3 program package in Materials Studio 4.4 [41,42].

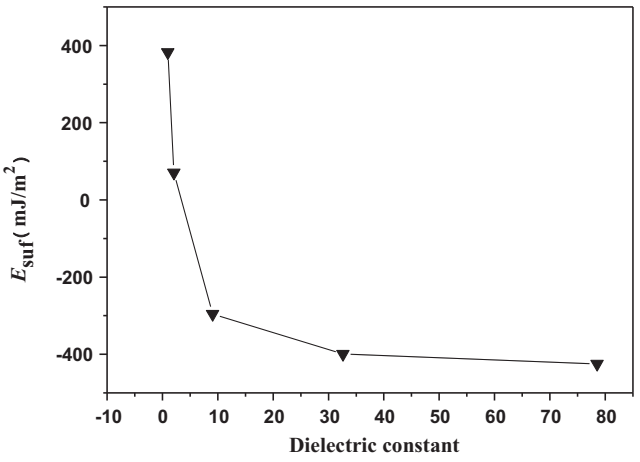

Fig. 2. The surface energies of $Cu_2O(1\,1\,1)$ surface with different dielectric constants.

3. Results and discussion

3.1. Calculations of CO molecules and bulk Cu_2O

The obtained values verify the credibility of the selected calculation method: firstly, the bond length, bond dissociation energy and stretching frequency of molecular CO calculated from our approach are r(C–O) = 0.1143 nm, E_{BDE} = 1091.24 kJ mol^{-1} and ν_{C-O} = 2128 cm^{-1}, respectively, which are in good agreement with the experimental values of 0.1128 nm [43], 1076.38 ± 0.67 kJ mol^{-1} [44] and ν_{C-O} = 2138 cm^{-1} [20], respectively, as well as with other similar GGA results [19]. Then, the next test is to predict the lattice constant of bulk Cu_2O. The calculated value for the lattice constant is 0.4430 nm, which is close to the experimental value of 0.4270 nm [45,46]. Such results obtained in these tests make us confident in the research about the adsorption of CO on $Cu_2O(1\,1\,1)$ surface.

3.2. Surface energies of $Cu_2O(1\,1\,1)$ surface

In order to understand the stability and relevant orientations of the $Cu_2O(1\,1\,1)$ surface in different environments, we studied the surface energies of $Cu_2O(1\,1\,1)$ surface in vacuum, liquid paraffin, methylene chloride, methanol and water. The surface energy of $Cu_2O(1\,1\,1)$ surface [47,48] calculated in vacuum is defined as:

$$E_{suf} = \frac{E_{Cu_2O(1\ 1\ 1)} - E_{bulk}}{2S_{Cu_2O(1\ 1\ 1)}} \quad (1)$$

Here E_{suf} is the surface energy of $Cu_2O(1\,1\,1)$ surface, $E_{Cu_2O(1\ 1\ 1)}$ and E_{bulk} are the total energy of $Cu_2O(1\,1\,1)$ surface in vacuum and the bulk phase of Cu_2O containing the same number of atoms as

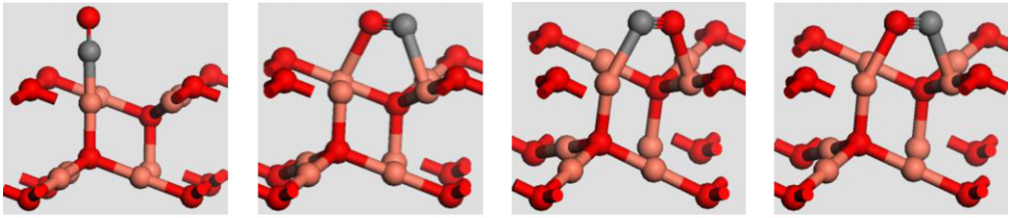

Fig. 3. Different adsorption models of CO on $Cu_2O(1\,1\,1)$ surface. Grey, red and orange balls stand for C, O and Cu atoms throughout the paper. (For interpretation of the references to color in this figure legend, the reader is referred to the web version of the article.)

in the slab, and $S_{Cu_2O(1\ 1\ 1)}$ is the surface area of $Cu_2O(1\,1\,1)$. The surface energies E_{suf} in other environments are also calculated by Eq. (1).

According to Eq. (1), the surface energies in different solvent environments are plotted in Fig. 2 as functions of the solvent dielectric constant. Fig. 2 shows that the surface energies of $Cu_2O(1\,1\,1)$ decrease as the dielectric constants increase. When the dielectric constant changes from vacuum ($\varepsilon = 1$) to methylene chloride ($\varepsilon = 9.08$), the values of surface energies change rapidly. However, when the dielectric constant is equal to or greater than 32.63, the effect of solvent on the $Cu_2O(1\,1\,1)$ surface energies is not obvious.

For a nanocrystallite of a given volume, the Gibbs–Curie–Wulff law [48] allows the morphology to be determined by applying the following relationship:

$$\frac{E_{suf}}{d_{1\ 1\ 1}} = \text{constant} \tag{2}$$

$$V = \frac{S_{Cu_2O(1\ 1\ 1)} d_{1\ 1\ 1}}{3} \tag{3}$$

Here $d_{1\,1\,1}$ is the length of the normal line to the 1 1 1 face from Wulff's point in the crystal, and the pyramid with the base of the 1 1 1 face and the height of $d_{1\,1\,1}$ has a total volume V, which is held tightly.

According to Eqs. (2) and (3), we can see that the smaller the surface energy is, the larger the surface area is, so the $Cu_2O(1\,1\,1)$ surface area in solvent is larger than that in vacuum. Namely, when the dielectric constants changes from vacuum ($\varepsilon = 1$) to methylene chloride ($\varepsilon = 9.08$), the surface area increases rapidly, and becomes stable for higher values of $\varepsilon = 32.63$. In addition, Mulliken charges for the relaxed top 3-layer of $Cu_2O(1\,1\,1)$ surface, as shown in Fig. 1, are analyzed. The calculated results show that the charges of the relaxed top 3-layer surface decrease with the solvent polarity increasing. The order is as follows: $\varepsilon = 1$ ($-0.035\,e$) > $\varepsilon = 2.06$ ($-0.048\,e$) > $\varepsilon = 9.08$ ($-0.089\,e$) > $\varepsilon = 32.63$ ($-0.141\,e$) > $\varepsilon = 78.54$ ($-0.154\,e$), suggesting that $Cu_2O(1\,1\,1)$ surface have the polarization of electron induced by the solvent effect.

The above results show that solvent environment can improve the stability of $Cu_2O(1\,1\,1)$ surface and will favor the $Cu_2O(1\,1\,1)$ surface area growth. Furthermore, the solvent effect induces the electron polarization of $Cu_2O(1\,1\,1)$ leading to the improvement of the catalytic activity. In order to probe into theses facts and to determine whether solvent can improve the catalytic activity of $Cu_2O(1\,1\,1)$ surface, we will study the adsorption of CO on $Cu_2O(1\,1\,1)$ surface both in vacuum and in solvents, as follows.

3.3. CO adsorption on $Cu_2O(1\,1\,1)$ in vacuum

The adsorption energy is defined as $E_{ads} = E_{CO} + E_{Cu_2O(1\ 1\ 1)} - E_{CO/Cu_2O(1\ 1\ 1)}$, where the first term is the total energy of the CO molecule, the second term is the total energy of the $Cu_2O(1\,1\,1)$ slab, and the third term is the total energy for the slab with the adsorbed CO on the surface. Therefore, a positive E_{ads} value means a more favorable structure.

For the adsorption of CO on $Cu_2O(1\,1\,1)$ surface, the CO molecule is allowed to approach $Cu_2O(1\,1\,1)$ surface along two adsorption modes: one is an end-on mode involving CO perpendicular to the surface (M1) over four distinct sites, the other is a side-on mode involving CO parallel to the surface (M2–M4). The geometries used in the calculations are presented in Fig. 3.

For the end-on mode of CO adsorption over four distinct sites, the calculated results show that the adsorptions of C-down configuration are much stronger than those of O-down. Meanwhile, the adsorption energies of CO adsorbed with C-down over Cu_{CSA}, O_{SUF} and O_{SUB} are 221.7, 214.5 and 176.5 kJ mol^{-1}, respectively. CO adsorbed with C-down over Cu_{CUS} site has the largest adsorption energy (327.0 kJ mol^{-1}), suggesting that CO adsorbed with C-down over Cu_{CUS} site is the most stable configuration among all the end-on modes of CO adsorption over four distinct sites. In the optimized structure of CO adsorbed with C-down over Cu_{CUS} site, the C–O and Cu–C bond lengths are 0.1148 and 0.1839 nm, respectively. And the angle of O–C–Cu_{CUS} is 178.3°. The C–O bond length 0.1148 nm is longer than the corresponding length 0.1128 nm for the free CO molecule, which indicates that the intensity of C–O bond is weakened and that the C–O bond is activated. The electron transfer from CO to substrate as the C atom bind to the Cu_{CUS} site and the net charge of CO is 0.388 e. For the side-on mode of CO adsorption, the optimized M2 structure is converted to M1 mode with C-down over Cu_{CSA} site. The optimized structure of M3 mode is converted to M1 mode with C-down over Cu_{CUS} site. But in the optimized structure of M4 mode, CO still lies flatly over bridge; in this structure the C and O atoms of CO bind with the Cu_{CSA} and Cu_{CUS} atoms, respectively. The C–O bond length is 0.1170 nm and the Cu_{CUS}–O and Cu_{CSA}–C bond lengths are 0.2214 and 0.2168 nm, respectively, and the corresponding adsorption energies is 203.1 kJ mol^{-1}.

The above results show that the end-on mode of CO adsorption with C-down over Cu_{CUS} site has the larges adsorption energy among all adsorption modes and that it is the most stable configuration for CO adsorption on $Cu_2O(1\,1\,1)$ surface, these conclusions are in agreement with some reported studies [20–24].

3.4. CO adsorption on $Cu_2O(1\,1\,1)$ in solvent

To understand more deeply the solvent effect on CO adsorption and activation over $Cu_2O(1\,1\,1)$ surface in solvent, we have investigated the end-on mode of CO adsorption with C-down over Cu_{CUS} site of $Cu_2O(1\,1\,1)$ surface in four types of solvents; liquid paraffin, methylene chloride, methanol and water. The values of the most relevant structural parameters and Mulliken charge for the stable structure of CO with C-down adsorbed over Cu_{CUS} site of $Cu_2O(1\,1\,1)$ surface are presented in Table 1.

Firstly, the adsorption energies are plotted in Fig. 4 as functions of the solvent dielectric constant; the result shows that all the adsorption models are stabilized when the solvent dielectric

Table 1
Calculated geometrical structural parameters, adsorption energies and Mulliken charges of CO adsorbed over Cu_{CUS} site of $Cu_2O(1\,1\,1)$ surface in four types of solvents.

Parameters	Vacuum	Liquid paraffin	Methylene chloride	Methanol	Water
$d_{(C-O)}$/nm	0.1148	0.1154	0.1168	0.1176	0.1178
$d_{(Cu-C)}$/nm	0.1839	0.1831	0.1817	0.1812	0.1809
α/°	178.3	177.7	174.8	173.2	173.6
q_C	0.486	0.466	0.418	0.388	0.382
q_O	−0.098	−0.141	−0.221	−0.260	−0.270
q_{CO}	0.388	0.325	0.197	0.128	0.112
$q_{Cu_2O(1\ 1\ 1)}$	−0.388	−0.325	−0.197	−0.128	−0.112
E_{ads}/kJ mol^{-1}	327.0	777.4	1312.6	1472.5	1507.9

constant increases. In the considered values of ε, vacuum is stabilized by 327.0 kJ mol^{-1}, liquid paraffin by 777.4 kJ mol^{-1}, methylene chloride by 1312.6 kJ mol^{-1}, methanol by 1472.5 kJ mol^{-1} and water by 1507.9 kJ mol^{-1}, respectively. The adsorption energies vary mainly for dielectric constant values ranging from $\varepsilon = 1$ to $\varepsilon = 9.08$, with only small changes remaining for the higher values $\varepsilon = 32.63$. The increase of adsorption energies show that the solvent improves the stability of CO adsorption on $Cu_2O(1\,1\,1)$ surface.

Next, the C–O and Cu–C bond lengths are analyzed and plotted in Fig. 5 as functions of the solvent dielectric constant. As shown in Fig. 5(a), the C–O bond length increases obviously when ε is in the range from 1 to 9.08, and the change of the C–O bond length is not obvious when ε is equal to or greater than 32.63. The elongation of the C–O bond indicates that the solvent induces the higher activation of the C–O bond than that in vacuum and this weakens the intensity of the C–O bond. And the Cu–C bond length decreases when ε varies from 1 to 9.08, then remains stable for higher values of $\varepsilon = 32.63$ (see Fig. 5(b)). The smaller the Cu–C bond length is, the more stable the adsorption system is, which is in good accordance with the results obtained from the adsorption energy. In a solvent, the bond angle α changes little. Finally, CO adsorbed on $Cu_2O(1\,1\,1)$ surface is detected to be non-dissociative adsorption in either vacuum or solvent by using the monitor bonding in Dmol^3. The above results show that the solvent not only favors the stability of CO adsorption, but also largely induces the C–O bond activation. In addition, in order to verify the solvent effect on the stretching of the C–O bond lengths, we also investigated the adsorption process of CO molecule on $Cu_2O(1\,1\,1)$ surface in different solvents, including pure physisorption at a relatively large distance from the $Cu_2O(1\,1\,1)$ surface (typically $d > 0.3$ nm) and chemisorption where chemical bond formation between CO and the Cu_{CUS} over $Cu_2O(1\,1\,1)$ surface can occur. A notable amount of time was spent on studying the transition state induced by the solvent in the adsorption process. However, since the potential energy decreases at all times in the curve of potential energies, there is no transition state induced by the solvent for the adsorption process of CO molecule approaching the $Cu_2O(1\,1\,1)$ surface in different solvents.

Further, to understand the relationship between the electron transfer and the solvent effect, we also calculated Mulliken charges of the CO adsorbed on the Cu_2O $(1\,1\,1)$ surface in different solvents. As listed in Table 1, it can be seen that the adsorbed CO molecules are positively charged, which indicates that electron transfer occurs from CO to $Cu_2O(1\,1\,1)$ surface. Meanwhile, Mulliken charges of C, O and CO decrease with the increase of solvent polarity, as shown in Fig. 6. However, the $Cu_2O(1\,1\,1)$ surface obtains the electrons, and the charges of $Cu_2O(1\,1\,1)$ surface increase with the increase of solvent polarity. The above results show that the solvent effect has the opposite influencing trend for adsorbed CO and $Cu_2O(1\,1\,1)$ surface, which means that the polarization between CO molecule and $Cu_2O(1\,1\,1)$ surface decreases with the increase of solvent polarity.

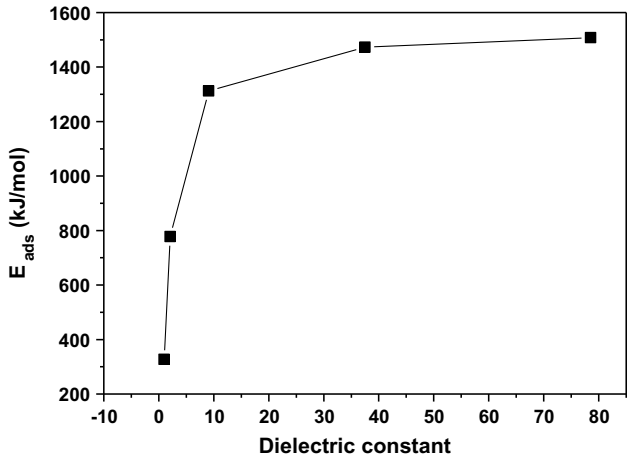

Fig. 4. The change of the adsorption energy for CO adsorbed over Cu_{CUS} site of $Cu_2O(1\,1\,1)$ surface with variable dielectric constant of the solvent.

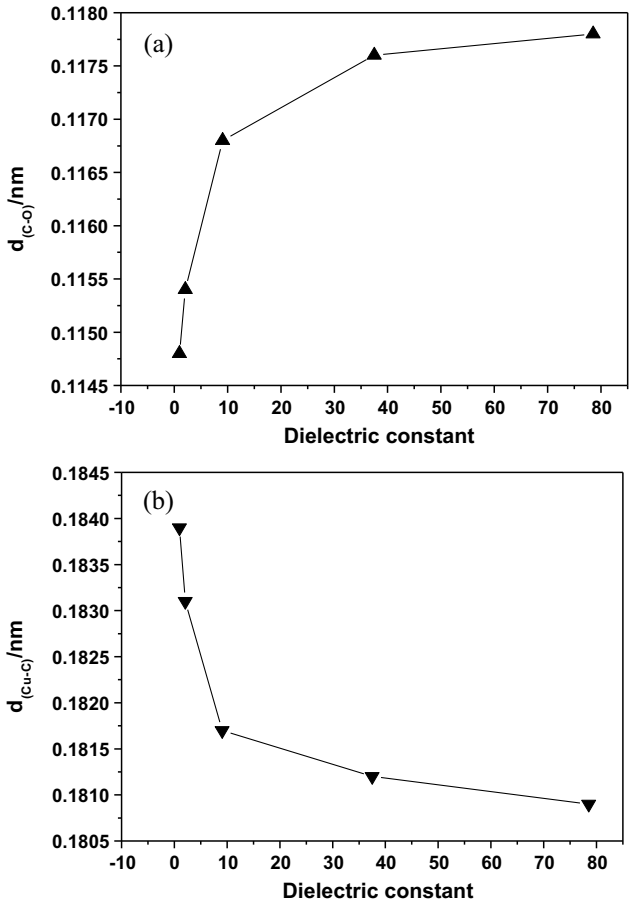

Fig. 5. The change of C–O and Cu–C bond lengths for CO adsorbed over Cu_{CUS} site of $Cu_2O(1\,1\,1)$ surface with variable dielectric constant of the solvent.

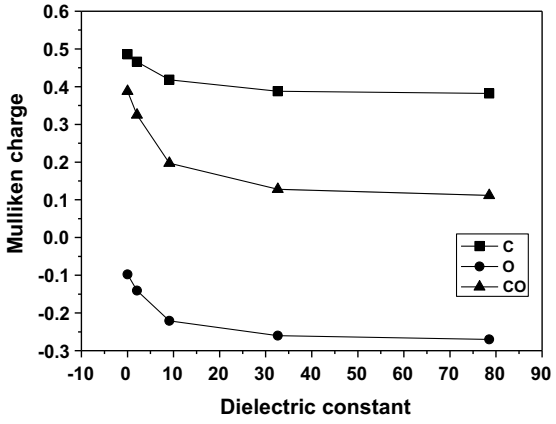

Fig. 6. Mulliken charges of C, O and CO of CO adsorbed on $Cu_2O(1\,1\,1)$ surface with different dielectric constants.

Therefore, when CO is adsorbed on $Cu_2O(1\,1\,1)$ surface in different solvents, the solvent effect can work to stabilize the polarization and will favor the adsorption of CO. Moreover, the elongation of the C–O bonds increase with the Mulliken charge of C, O and CO decreasing, such a trend indicates that the stronger electron transfer from the surface into the anti bonding orbital of CO induces the higher activation of the C–O bonds.

Finally, the C–O stretching frequencies in vacuum and different solvents are calculated, as shown in Table 2. The calculated C–O stretching frequency $\nu_{(C-O)}$ for free CO molecule is $\nu_0 = 2128\,cm^{-1}$, and the experimental value is $\nu = 2138\,cm^{-1}$ in Section 3.1, which suggests that some discrepancy exists between the calculated and experimental values. So an emendation factor $\alpha = \nu/\nu_0$ [49] is introduced to revise the calculated C–O stretching frequency. As shown in Table 2, a red-shift ($54\,cm^{-1}$) of the C–O stretching frequencies is calculated for CO adsorption on $Cu_2O(1\,1\,1)$ surface in vacuum. With the dielectric constants ε increasing, the C–O stretching frequency decreases obviously for liquid paraffin and methylene chloride by 108 and $209\,cm^{-1}$, as well as decreasing slowly for methanol and water by 266 and $281\,cm^{-1}$, respectively. Although there are no experimental data available for comparison with our calculated C–O stretching frequencies of CO adsorption on $Cu_2O(1\,1\,1)$ surface in different solvents, the calculated C–O stretching frequencies accord well with these from the previous theoretical studies by Chen et al. [50], which show the red-shift ($50\,cm^{-1}$) of $\nu_{(C-O)}$ upon coordination of CO on $Cu_2O(1\,1\,1)$ in vacuum. Therefore, we think the calculated results of CO adsorption on $Cu_2O(1\,1\,1)$ surface in different solvents are reasonable. Furthermore, we hope that some experiments will be performed to confirm the calculated C–O stretching frequency in our future work. The red-shift of the C–O stretching frequency indicates that the intensity of C–O bond decreases; these results are in line with the results obtained from the C–O bond length.

Table 2
Calculated C–O stretching frequencies of CO adsorbed on $Cu_2O(1\,1\,1)$ surface in different solvent systems.

	ν/cm^{-1}		$\Delta\nu/cm^{-1}$	
	$\alpha = 1$	$\alpha = 0.9953$	$\alpha = 1$	$\alpha = 0.9953$
Free CO	2138	2128	0	0
Vacuum	2084	2074	−54	−54
Liquid paraffin	2030	2020	−108	−108
Methylene chloride	1929	1920	−209	−208
Methanol	1872	1863	−266	−265
Water	1857	1848	−281	−280

Based on the above calculated results, we can claim that the structural parameters, stretching frequencies and adsorption energies of CO adsorbed on $Cu_2O(1\,1\,1)$ surface change rapidly when dielectric constants change from 1 to 9.08, and are stable for higher values of $\varepsilon = 32.63$, which is in line with the change trends of $Cu_2O(1\,1\,1)$ surface energy when ε varies from 1 to 78.54. Meanwhile, the solvent environment reduces the $Cu_2O(1\,1\,1)$ surface energy and favors the $Cu_2O(1\,1\,1)$ surface area growth, which means that solvent improves the stability of the $Cu_2O(1\,1\,1)$ surface. The increasing adsorption energy of CO shows that solvent is propitious to the adsorption of CO on $Cu_2O(1\,1\,1)$ surface. And the elongation of C–O bond suggests that $Cu_2O(1\,1\,1)$ in solvent shows higher catalytic performance for CO activation, namely, the solvent can improve the catalytic activity of $Cu_2O(1\,1\,1)$ surface.

3.5. The role of solvent for the CO adsorption on $Cu_2O(1\,1\,1)$ in solvent

Considering that solvent molecules may also interact with $Cu_2O(1\,1\,1)$ surface, we have also studied the role of solvent for the CO adsorption on $Cu_2O(1\,1\,1)$ surface in solvent; such study is based on the adsorption of solvent molecules on $Cu_2O(1\,1\,1)$ surface. For liquid paraffin, as it is a complicated compound with the main component of linear alkyl C_nH_{2n+2} ($n = 18$–24), C_3H_8, a segment of the linear alkyl C_nH_{2n+2} [35], is chosen to investigate the interaction of liquid paraffin with $Cu_2O(1\,1\,1)$ surface.

The results in the earlier Section 3.3 and in previous reports [20–24] have shown that Cu_{CUS} is the most advantageous adsorption site and that Cu_{CUS} sites comprise coordinatively unsaturated Cu^+ cations. Therefore, only Cu_{CUS} is considered for the adsorption of four solvent molecules on $Cu_2O(1\,1\,1)$ surface. In the optimized structures, C_3H_8 and CH_2Cl_2 molecules are both inclined to keep away from the surface, while CH_3OH and H_2O are still adsorbed at Cu_{CUS} sites. The corresponding adsorption energies of C_3H_8, CH_2Cl_2, CH_3OH and H_2O at Cu_{CUS} site are 220.1, 263.2, 294.9 and $295.6\,kJ\,mol^{-1}$, respectively. Combining with the adsorption energy of CO on $Cu_2O(1\,1\,1)$ in different solvents presented in Table 1, we can find that the interaction of solvent molecule with $Cu_2O(1\,1\,1)$ surface is far less than that of CO with $Cu_2O(1\,1\,1)$ in this solvent environment; for example, the adsorption energy of liquid paraffin on $Cu_2O(1\,1\,1)$ is $220.1\,kJ\,mol^{-1}$, but the adsorption energy of CO on $Cu_2O(1\,1\,1)$ increases obviously from $327.0\,kJ\,mol^{-1}$ in vacuum to $777.4\,kJ\,mol^{-1}$ in liquid paraffin. The increasing value of the adsorption energy is $450.4\,kJ\,mol^{-1}$, which is still far larger than that of liquid paraffin on $Cu_2O(1\,1\,1)$. And the adsorption energy of CH_3OH with $Cu_2O(1\,1\,1)$ is $294.9\,kJ\,mol^{-1}$, but the adsorption energy of CO on $Cu_2O(1\,1\,1)$ changes obviously from $327.0\,kJ\,mol^{-1}$ in vacuum to $1472.5\,kJ\,mol^{-1}$ in methanol. The increasing values of the adsorption energy is $1145.5\,kJ\,mol^{-1}$. In like manner, CH_2Cl_2 and H_2O have the consistent change trend.

Such results about the interaction of solvent molecules with $Cu_2O(1\,1\,1)$ surface suggest that solvent molecules, such as liquid paraffin, methylene chloride, methanol and water, basically contribute the increase of adsorption energy for the CO adsorption on $Cu_2O(1\,1\,1)$ surface in solvent. This suggests that solvent molecules primarily play the role of solvent and show strong solvent effects for the adsorption of CO on $Cu_2O(1\,1\,1)$ surface in solvent. Therefore, it is concluded that the solvent effect is the dominating cause for the enhancement of CO interaction with $Cu_2O(1\,1\,1)$ in solvent, in which $Cu_2O(1\,1\,1)$ shows higher catalytic performance for C–O bond activation. But the solvent effect may be not the only reason promoting CO activation. Furthermore, the above results also suggest that COSMO can well reflect the solvent effect on the CO adsorption over the $Cu_2O(1\,1\,1)$ surface.

4. Conclusions

The density functional theory (DFT) combined with conductor-like solvent model (COSMO) is applied to study the $Cu_2O(1\,1\,1)$ surface properties in different solvents and the adsorption of CO on $Cu_2O(1\,1\,1)$. According to the Gibbs–Curie–Wulff law, when the dielectric constant changes from vacuum (1) to methylene chloride (9.08), the surface area changes rapidly, and the area becomes stable for higher value of $\varepsilon = 32.63$. The solvent environment favors $Cu_2O(1\,1\,1)$ surface area growth. On the basis of the adsorption energies and C–O bond length, Cu_{CUS} is the most stable site for CO adsorption. The abilities of CO adsorption and activation on $Cu_2O(1\,1\,1)$ are in the same order: water ($\varepsilon = 78.54$) methanol ($\varepsilon = 32.63$) methylene chloride ($\varepsilon = 9.08$) liquid paraffin ($\varepsilon = 2.06$) vacuum ($\varepsilon = 1$), and the adsorption of CO on $Cu_2O(1\,1\,1)$ surface is exothermic. Meanwhile, the solvent effects can effectively improve the stability and the catalytic activity of $Cu_2O(1\,1\,1)$ surface.

Acknowledgements

The authors thank anonymous reviewers for their helpful suggestions on the quality improvement of our present paper. And the authors gratefully acknowledge the financial support of this work by the National Natural Science Foundation of China (Grant Nos. 20906066, 20976115 and 20976113).

References

[1] D.F. Jin, B. Zhu, Z.Y. Hou, J.H. Fei, H. Lou, X.M. Zheng, Fuel 86 (2007) 2707–2713.
[2] K.P. Sun, W.W. Lu, F.Y. Qiu, S.W. Liu, X.L. Xu, Appl. Catal. A: Gen. 252 (2003) 243–249.
[3] J.H. Kim, M.J. Park, S.J. Kim, O.S. Joo, K.D. Jung, Appl. Catal. A: Gen. 264 (2004) 37–41.
[4] G.C. Chinchen, K.C. Waugh, J. Catal. 97 (1986) 280–283.
[5] W.R.A.M. Robinson, J.C. Mol, Appl. Catal. 63 (1990) 165–179.
[6] Y.W. Suh, S.H. Moon, H.K. Rhee, Catal. Today 63 (2000) 447–452.
[7] B.B. Breman, A.A.C.M. Beenackers, H.A. Schuurman, E. Oesterholt, Catal. Today 24 (1995) 5–14.
[8] M.W.E.V.D. Berg, S. Polarz, O.P. Tkachenko, K.V. Klementiev, M. Bandyopadhyay, L. Khodeir, H. Gies, M. Muhler, W. Grünert, J. Catal. 241 (2006) 446–455.
[9] J. Nerlov, S. Scker, J. Wambach, I. Chorkendorff, Appl. Catal. A: Gen. 191 (2000) 97–109.
[10] H. Orita, S. Naito, K. Tamaru, J. Catal. 90 (1984) 183–193.
[11] T. Fukunaga, N. Ryumon, S. Shimazu, Appl. Catal. A: Gen. 348 (2008) 193–200.
[12] R.Q. Yang, X.C. Yu, Y. Zhang, W.Z. Li, N. Tsubaki, Fuel 87 (2008) 443–450.
[13] H. Nishimura, T. Yatsu, T. Fujitani, T. Uchijima, J. Nakamura, J. Mol. Catal. A: Chem. 155 (2000) 3–11.
[14] C.S. Chen, J.H. You, J.H. Lin, C.R. Chen, K.M. Lin, Catal. Commun. 9 (2008) 1230–1234.
[15] G.R. Sheffer, T.S. King, J. Catal. 115 (1989) 376–387.
[16] Y. Kanai, T. Watanabe, T. Fujitani, T. Uchijima, J. Nakamura, Catal. Lett. 38 (1996) 157–163.
[17] R.G. Herman, K. Klier, G.W. Simmons, B.P. Finn, J.B. Bulko, T.P. Kobylinski, J. Catal. 56 (1979) 407–429.
[18] G.C. Chinchen, P.J. Denny, J.R. Jennings, M.S. Spencer, K.C. Waugh, Appl. Catal. 36 (1988) 1–65.
[19] Z.J. Zuo, W. Huang, P.D. Han, Z.H. Li, Appl. Surf. Sci. 256 (2010) 2357–2362.
[20] B.Z. Sun, W.K. Chen, J.D. Zheng, C.H. Lu, Appl. Surf. Sci. 255 (2008) 3141–3148.
[21] M. Casarin, C. Maccato, A. Vittadini, Chem. Phys. Lett. 280 (1997) 53–58.
[22] T. Bredow, A.M. Márquez, G. Pacchioni, Surf. Sci. 430 (1999) 137–145.
[23] M. Casarin, A. Vittadini, Surf. Sci. 387 (1997) 1079–1084.
[24] T. Bredow, G. Pacchioni, Surf. Sci. 373 (1997) 21–32.
[25] E.F. de Lima, J.W. de M. Carneiro, C. Fenollar-Ferrer, S. Miertus, S. Zinoviev, N.C. Om Tapanes, D.A.G. Aranda, Fuel 89 (2010) 685–690.
[26] J. Sebek, Z. Kejik, P. Bour, J. Phys. Chem. A 110 (2006) 4702–4711.
[27] N. Sanna, G. Chillemi, A. Grandi, S. Castelli, A. Desideri, V. Barone, J. Am. Chem. Soc. 127 (2005) 15429–15436.
[28] J. Tomasi, B. Mennucci, R. Cammi, Chem. Rev. 105 (2005) 2999–3093.
[29] A. Klamt, G. Schrmann, J. Chem. Soc. Perkin Trans. 2 (1993) 799–805.
[30] P. Imhof, S. Fischer, R. Krämer, J.C. Smith, J. Mol. Struct. (Theochem) 713 (2005) 1–5.
[31] T. Todorova, B. Delley, Mol. Simul. 34 (2008) 1013–1017.
[32] A.V. Gavrilenko, T.D. Matos, C.E. Bonner, S.S. Sun, C. Zhang, V.I. Gavrilenko, J. Phys. Chem. C 112 (2008) 7908–7912.
[33] R.G. Zhang, L.X. Ling, B.J. Wang, W. Huang, Appl. Surf. Sci. 256 (2010) 6717–6722.
[34] M.M. Islam, B. Diawara, V. Maurice, P. Marcus, J. Mol. Struct. (THEOCHEM) 903 (2009) 41–48.
[35] K.H. Schulz, D.F. Cox, Phys. Rev. B 43 (1991) 1610–1621.
[36] R.G. Zhang, B.J. Wang, L.X. Ling, H.Y. Liu, W. Huang, Appl. Surf. Sci. 257 (2010) 1175–1180.
[37] A.D. Becke, J. Chem. Phys. 88 (1988) 2547–2553.
[38] C. Lee, W. Yang, R.G. Parr, Phys. Rev. B 37 (1988) 785–789.
[39] Y. Inada, H. Orita, J. Comput. Chem. 29 (2008) 225–232.
[40] X. Wang, W.K. Chen, C.H. Lu, Appl. Surf. Sci. 254 (2008) 4421–4431.
[41] B. Delley, J. Chem. Phys. 92 (1990) 508–517.
[42] B. Delley, J. Chem. Phys. 113 (2000) 7756–7764.
[43] J.X. Shao, X.L. Cheng, X.D. Yang, F.P. Zhang, S.H. Ge, J. At. Mol. Phys. 23 (2006) 80–84.
[44] Y.R. Luo, Handbook of Bond Dissociation Energies in Organic Compounds, Science Press, Beijing, 2005, p. 209.
[45] R. Restori, D. Schwarzenbach, Acta Crystallogr. B 42 (1986) 201–208.
[46] M.A. Nygren, L.G.M. Pettersson, J. Phys. Chem. 100 (1996) 1874–1878.
[47] P. Raybaud, M. Digne, R. Iftimie, W. Wellens, P. Euzen, H. Toulhoat, J. Catal. 201 (2001) 236–246.
[48] Z.J. Zuo, L.L. Sun, W. Huang, P.D. Han, Z.H. Li, Appl. Catal. A: Gen. 375 (2010) 181–187.
[49] B.Z. Sun, W.K. Chen, S.H. Liu, M.J. Cao, C.H. Lu, Y. Xu, Chin. J. Inorg. Chem. 22 (2006) 1215–1221.
[50] B.Z. Sun, W.K. Chen, Y. Li, C.H. Lu, Chin. J. Struct. Chem. 28 (2009) 311–314.